Environment International 185 (2024) 108538

Contents lists available at ScienceDirect

Environment International

journal homepage: www.elsevier.com/locate/envint

Full length article

# Bacterial communities of planktonic bacteria and mature biofilm in service lines and premise plumbing of a Megacity: Composition, Diversity, and influencing factors

Anran Ren [a,b,c,1], Mingchen Yao [a,b,c,1], Jiaxing Fang [a,d], Zihan Dai [a,e], Xiaoming Li [a,c,*], Walter van der Meer [d,f], Gertjan Medema [f,g,h], Joan B. Rose [h], Gang Liu [a,b,c,*]

[a] Key Laboratory of Drinking Water Science and Technology, Research Centre for Eco-Environmental Sciences, Chinese Academy of Sciences, Beijing 100085, China
[b] Sanitary Engineering, Department of Water Management, Faculty of Civil Engineering and Geosciences, Delft University of Technology, P.O. Box 5048, 2600 GA Delft, The Netherlands
[c] University of Chinese Academy of Sciences, Beijing, China
[d] Science and Technology, University of Twente, P.O. Box 217, 7500AE Enschede, The Netherlands
[e] School of Civil and Environmental Engineering, Georgia Institute of Technology, Atlanta, GA 30332, USA
[f] Oasen Drinkwater, PO Box 122, 2800 AC, Gouda, The Netherlands
[g] KWR Watercycle Research Institute, P.O. Box 1072, 3430 BB Nieuwegein, The Netherlands
[h] Department of Fisheries and Wildlife, Michigan State University, East Lansing, MI 48823, USA

ARTICLE INFO

*Keywords:*
Service lines
Premise plumbing
Bacterial community
Biofilm
Pipe ages
Pipe material

ABSTRACT

Although simulated studies have provided valuable knowledge regarding the communities of planktonic bacteria and biofilms, the lack of systematic field studies have hampered the understanding of microbiology in real-world service lines and premise plumbing. In this study, the bacterial communities of water and biofilm were explored, with a special focus on the lifetime development of biofilm communities and their key influencing factors. The 16S rRNA gene sequencing results showed that both the planktonic bacteria and biofilm were dominated by Proteobacteria. Among the 15,084 observed amplicon sequence variants (ASVs), the 33 core ASVs covered 72.8 %, while the 12 shared core ASVs accounted for 62.2 % of the total sequences. Remarkably, it was found that the species richness and diversity of biofilm communities correlated with pipe age. The relative abundance of ASV2 (f_Sphingomonadaceae) was lower for pipe ages 40–50 years (7.9 %) than for pipe ages 10–20 years (59.3 %), while the relative abundance of ASV10 (f_Hyphomonadaceae) was higher for pipe ages 40–50 years (19.5 %) than its presence at pipe ages 20–30 years (1.9 %). The community of the premise plumbing biofilm had significantly higher species richness and diversity than that of the service line, while the steel-plastics composite pipe interior lined with polyethylene (S-PE) harbored significantly more diverse biofilm than the galvanized steel pipes (S-Zn). Interestingly, S-PE was enriched with ASV27 (g_*Mycobacterium*), while S-Zn pipes were enriched with ASV13 (g_*Pseudomonas*). Moreover, the network analysis showed that five rare ASVs, not core ASVs, were keystone members in biofilm communities, indicating the importance of rare members in the function and stability of biofilm communities. This manuscript provides novel insights into real-world service lines and premise plumbing microbiology, regarding lifetime dynamics (pipe age 10–50 years), and the influences of pipe types (premise plumbing vs. service line) and pipe materials (S-Zn vs. S-PE).

## 1. Introduction

A continuous supply of safe and high-quality drinking water is essential for modern cities. As an important barrier protecting drinking water from contamination, the drinking water network system (e.g., distribution main pipe; service line; premise plumbing) can be tens of hundreds of kilometers long, within which biological quality deterioration has been widely reported worldwide (Fanget al., 2023; Lautenschlageret al., 2010; Liuet al., 2017b; Prestet al., 2016). Compared to with distribution main pipe (D = 63–110 mm), service line

* Corresponding authors at: Research Center for Eco-Environmental Sciences, Chinese Academy of Sciences, China.
*E-mail addresses:* xmli@rcees.ac.cn (X. Li), gliu@rcees.ac.cn, g.liu-1@tudelft.nl (G. Liu).
[1] Anran Ren and Mingchen Yao contributed equally to this manuscript.

https://doi.org/10.1016/j.envint.2024.108538
Received 28 December 2023; Received in revised form 14 February 2024; Accepted 26 February 2024
Available online 28 February 2024

(D = 25–40 mm) and premise plumbing (D = 20–25 mm) typically have low disinfectant concentration, long residence times and high surface area to volume ratio, which can favor unwanted bacterial growth and biofilm formation (Fanget al., 2023; Lautenschlageret al., 2010; Linget al., 2018; Liuet al., 2017a). Previous studies have confirmed service line and premise plumbing were major contributor to water quality deterioration at customer ends (Fanget al., 2023; Liet al., 2022). Investigating the variations in communities of planktonic bacteria and biofilm and the key influencing factors in such systems is important for understanding and managing microbiological water quality at customer ends.

It is generally agreed that most microbes in drinking water system exist in pipe wall biofilms, which can protect microbes against disinfectants, harbor (opportunistic) pathogens, and continuously release microbes into bulk water (Costertonet al., 1995). Therefore, considerable research attention has been devoted to the physiochemical characteristics of biofilms, their origin and development, influencing factors, and interactions between water and biofilms (Doutereloet al., 2013; Martinyet al., 2003; Yanget al., 2000). However, most of the available knowledge was obtained by short-term studies with simulation systems due to the difficulties in obtaining biofilm samples from field drinking water network systems (Boe-Hansenet al., 2002; Doutereloet al., 2018; Simunicet al., 2020). The three-year simulation study by Martiny et al. suggested that several years may be required before establishment of a steady biofilm state, challenging the relevance of short-term simulation studies (Martinyet al., 2003). By comparing biofilms obtained in simulated (2–3 years) and field systems (50 + years), Aggarwal et al. found significantly different bacterial communities, further challenging the effectiveness of simulated experiments mimicking full-scale distribution systems (Aggarwalet al., 2018). Although the period of 2–3 years is already rather long for simulation studies, it is still too short compared to the regular drinking water network system service time of several decades.

Valuable knowledge has been obtained by the limited number of biofilm studies in full-scale operational drinking water system, for example, in chlorinated German system (Henneet al., 2012), chloraminated American systems (Gomez-Smithet al., 2015; Waaket al., 2018), chloraminated Singapore system (Cruzet al., 2020), and chloraminated Chinese systems (Baiet al., 2010; Liet al., 2016). In the small-scale German system (20 + years), biofilm sampling was conducted mainly within the Helmholtz Centre for Infection Research campus (7/8 samples) when a building was dismantled (Henneet al., 2012), while in the American system, biofilm was collected from 10 main water samples (48–129 years) in conjunction with routine replacement activities (Gomez-Smithet al., 2015). Both abovementioned studies found similar biofilm communities formed on different pipe materials. However, a previous study found that galvanized steel pipes had a higher richness than polyethylene pipes and that the two materials formed different microbial communities (Yuet al., 2010). Biomass levels in galvanized steel pipe are typically higher than in polyethylene pipe biofilm, as the rough surface is more conducive to microbial attachment (Assaidiet al., 2018; Papciaket al., 2019). In Singapore system, monochloramine residual gradient along the drinking water distribution systems (DWDSs) were found to drive and shape the microbial community assembly (Cruzet al., 2020), while focusing on opportunistic pathogens, Waak et al. found that residual chloramines had opposite effects on nontuberculous mycobacteria and *Legionella* spp. in the biofilm of drinking water system, residual chloramine may increase mycobacteria biomass but decrease *Legionella* spp. abundance (Waaket al., 2018). Liu et al. have performed several studies in unchlorinated Dutch systems focused on the 360°-radial distribution of biofilm and the comparison and interactions among water, loose deposits, and biofilm, especially during the disturbances induced by supply-water quality changes (Liuet al., 2017a; Liuet al., 2020). However, biofilm sampling substantially depends on the occurrence of pipe breakage/replacement, which has hardly been possible with rigorous scientific design. Alternatively, some studies install biofilm sampling sensors/devices in drinking water network system to facilitate biofilm sampling (Doutereloet al., 2016; Doutereloet al., 2017; Kitajimaet al., 2021). Such an approach is non-destructive, which could be used to study the dynamic of biofilm development. However, most of the studies were conducted for a short period (biofilm age < 18 months), which was too short compare to real world service lines and premise plumbing biofilm (decades). To date, critical knowledge about how the bacterial communities of mature biofilms develop over decades and what the key influencing factors are from the perspective over decades remains unknown.

The objective of this study is to investigate the bacterial communities of water and biofilm in the chlorinated drinking water distribution system of a megacity, with a special focus on the service lines and premise plumbing. This study targeted on research question of what are the impacts of pipe ages, pipe types, and pipe material on the bacterial communities of biofilm, particularly in field distribution system and over long-term (decades). For this purpose, 81 water (WA) samples and 97 biofilm (BF) samples were obtained from 33 locations in an area of 130 $km^2$ in Beijing. The biofilm samples covered different ages (pipe age 10–50 years), materials (galvanized steel pipes, S-Zn; and the steel-plastics composite pipe interior lined with polyethylene, S-PE), and types (service line, SL; and premise plumbing, PP).

## 2. Materials and methods

### 2.1. Study area

The sampling was conducted during the first week of November 2020 in the full scale chlorinated drinking water distribution system, with a special focus on the service lines and premise plumbing in Beijing, China. The residual chlorine concentrations in the finished water ranged 0.6–0.8 mg/L and at the sampling points 0.06–0.36 mg/L. At the drinking water treatment plant (DWTP), the source water is so called “south-water” from Yangtze River transported to Beijing, which is treated by pre-ozonation, coagulation, ozonation, carbon filtration, ultrafiltration, UV disinfection, and chlorination disinfection before the water is pumped into the distribution system. The DWDS has over 20,000 km of pipeline, covers an area of 1,300 $km^2$, and supplies drinking water to more than 18 million people, with a daily capacity of over 2.7 million $m^3$. In this study, a total of 81 water samples and 97 biofilm samples were taken from 33 locations in sub-areas of the DWDS (10–45 years, Figure S1, Table 1) that covers an area of 130 $km^2$ and supplied by the same drinking water treatment plant.

### 2.2. Sampling program

The sampling locations were not from all over the cities but mainly two regions. Sampling from locations with water only was combined with the regular sampling and monitoring program of the water utility as required by National Water Quality Regulations. The locations were fixed representative monitoring site decided based on population distribution in the area. Before taking water samples, each sampling tap was flushed until the water temperature remained stable for 30 s (~5 mins), water samples from DWDS. The tap was sterilized prior to sampling with 75 % alcohol. Sterilized glass bottles were used for taking water samples, 2 L water was filtrated by 0.2 μm filter for DNA extraction, and 0.2 L water was used for physiochemical parameter analysis. Triplicate samples were collected sequentially on the same day at each location, and in total 81 water samples were collected.

For sampling of biofilm and water paired samples, the locations were selected by the water utility combined with their microbial ecology survey program in the region. Biofilm samples were collected from service line (SL, DN 40/50) and premise plumbing (PP, DN 25). SL were the pipes connecting distribution mains to the residential building, which were sampled from water meter wells before entering residential buildings (pipes 20 cm above ground), while PP pipes were sampled

**Table 1**
Location and sampling information of water and biofilm.

| Location | Sample type | Sample quantity | Pipe material | Pipe type | Pipe age |
|---|---|---|---|---|---|
| L1 | WA | 3 | S-Zn | SL | 20–30 years (26) |
| | BF | 8 | | | |
| L2 | WA | 3 | S-Zn | SL | 30–40 years (31) |
| | BF | 8 | | | |
| L3 | WA | 3 | S-Zn | SL | 20–30 years (24) |
| | BF | 8 | | | |
| L4 | WA | 3 | S-Zn | SL | 40–50 years (45) |
| | BF | 8 | | | |
| L5 | WA | 3 | S-Zn | SL | 10–20 years (17) |
| | BF | 8 | | | |
| L6 | WA | 3 | S-PE | SL | 20–30 years (26) |
| | BF | 8 | | | |
| L7 | WA | 3 | S-Zn | PP | 20–30 years (27) |
| | BF | 3 | | | |
| L8 | WA | 3 | S-Zn | PP | 40–50 years (40) |
| | BF | 3 | | | |
| L9 | BF | 8 | S-Zn | SL | 30–40 years (33) |
| *L*10 | BF | 8 | S-Zn | SL | 30–40 years (30) |
| *L*11 | BF | 8 | S-Zn | SL | 20–30 years (20) |
| L12 | BF | 8 | S-Zn | SL | 30–40 years (31) |
| L13 | BF | 8 | S-PE | SL | 30–40 years (37) |
| L14 | BF | 3 | S-PE | SL | 10–20 years (10) |
| L15-L33 | WA | 3 × 19 | / | / | / |

from customers' kitchens. Before taking samples, the surrounding environment and pipe surfaces were disinfected by 75 % alcohol. Biofilm samples were collected by cutting pipe specimens (L = 20–30 cm) with a chop saw, the two open ends were sealed with sterile stoppers to prevent contamination and maintain moisture during transport, stored in sealed plastic bags.

For replicates, a minimum of 2 samples (duplicate) was taken when multiple taps or pipes in the neighborhood were available, while a minimum of 3 samples (triplicate) was taken when single location was sampled in the neighborhood. For SL, at each location (and its neighborhood), 4 pipes were taken and biofilm were sampled in duplicate in each pipe, which resulted in 8 samples per location/neighborhood (n = 2 × 4 = 8). For PP, 3 biofilm samples were taken from 3 pipes at each location (n = 1 × 3) = 3. In total, 97 biofilm samples were obtained from 14 locations.

At 8 locations (L1-L8), paired water and biofilm samples were collected (24 water samples, 54 biofilm samples). All samples were transported to the laboratory on ice within 6 h and processed 24 h after sampling. For biofilm samples, differences and potential influences of pipe ages (10–20 years, n = 8; 20–30 years, n = 24; 30–40 years, n = 32; 40–50 years, n = 8), pipe material (galvanized steel pipe, S-Zn, n = 72; steel-plastics composite pipe interior lined with polyethylene, S-PE, n = 19), and pipe types (service line, SL, n = 72; premise plumbing, PP, n = 6) were considered. For studying influences of pipe ages, 72 samples of the same pipe type (SL) and pipe material (S-Zn) were used; for comparing pipe material, 91 samples of the same pipe type (SL) were used; while for comparing pipe types, 78 samples of the same pipe material (S-Zn) were used.

### 2.3. Water chemistry measurement

Residual chlorine, temperature, pH, conductivity and dissolved oxygen (DO) were measured immediately after water samples were taken. The residual chlorine was measured using a DR300 spectrophotometer (HACH). Temperature, pH, conductivity and DO were measured using a muti-parameter water quality analyzer (Multi 3630, WTW, Germany). Total organic carbon was analyzed by a TOC analyzer (Shimadzu, Japan). The concentrations of iron (Fe), manganese (Mn), aluminum (Al), zinc (Zn) and copper (Cu) were determined by inductively coupled plasma-mass spectrometry (ICP-MS, Thermo Fisher Scientific, USA), the concentrations of calcium (Ca) and magnesium (Mg) were determined by inductively coupled plasma optical emission spectroscopy (ICP-OES, Shimadzu, Japan), and the concentrations of chloride ($Cl^-$), sulfate ($SO_4^{2-}$) and nitrite ($NO_3^-$) ions were determined by ion chromatography (IC, Dionex, USA), as described previously (Liuet al., 2014; Lytleet al., 2004; Penget al., 2010). Physicochemical characteristics of the water samples at each location are summarized in Table S1. Quality control samples, including laboratory fortified blanks and laboratory fortified samples, were analyzed after every ten samples.

### 2.4. Biomass collection and DNA extraction

Sterile rayon swabs (Copan, Brescia, Italy) were used to scrape the biofilm with an area of 50–60 $cm^2$ around the pipe wall at least 5 cm from a cut end to minimize the risk of biofilm disturbance or contamination from the chop saw. The swabs were stored at −20 °C until DNA extraction. DNA was recovered from filters or rayon swabs using a FastDNASPIN Kit (MP Biomedicals, United States) according to manufacturer's protocol (Wanget al., 2014). As negative controls, DNA was extracted from unused sterile rayon swabs (n = 3) and blank filters (n = 3). For planktonic bacteria, 2L of bulk water were filtered through 0.2-μm polycarbonate membrane filters (Whatman, UK) for each sample. The filters were preserved in sterile centrifuge tubes at −20 °C for subsequent DNA extraction.

### 2.5. qPCR analysis

qPCR assays targeting genes for total bacteria were performed by previously published method (Fiereret al., 2005; Huet al., 2012) as detailed in Table S2. The bacterial 16S rRNA gene were quantified by qPCR on a Quant Gene 9600 Real-Time PCR instrument (Bioer, China). Each 10 μL reaction contained: 5 μL of SsoFast EvaGreenSupermix (Bio-Rad), 0.8 μL of each primer (0.4 μM), 2.4 μL water and 1 μL of template DNA. PCR conditions for total 16S rRNA gene assays consisted of 40 cycles. Standard curves were created with serially diluted solutions containing custom gBlocks gene fragments. The oligonucleotides used for creating qPCR standard curves are summarized in Table S3. All qPCR runs for 16S rRNA genes included triplicate standard curves made up of serial dilutions ranging from $10^3$ copies/μL to $10^8$ copies/μL, triplicate negative controls, and triplicates of each sample being tested. Because of background amplification of 16S rRNA genes in reaction reagents, there was no limit of detection (LOD) for this assay, and the quantification limit (LOQ) for 16S rRNA genes qPCR assays was 1000 gene copies/reaction(Huet al., 2021). Amplification efficiencies, LOQs, LODs, and standard curves are summarized in Table S4.

### 2.6. Sequencing and data processing

Universal primers, forward 341F (5′-CCTACGGGNGGCWGCAG-3′) and reverse 785R (5′-GACTACHVGGGTATCTAATCC-3′), were used for PCR amplification (Yaoet al., 2023). The PCR products were detected by 2 % agarose gel electrophoresis and compared with the marker band, and 16S rRNA gene amplicon sequencing (paired-end 250 bp, Illumina NovaSeq) was performed on samples with suitable target bands of PCR products at Majorbio (Shanghai, China). Six negative controls and five biofilm samples at L14 did not have bands of PCR products, therefore, sequencing was not performed. The prime was removed with cutadapt 3.1 (Kechinet al., 2017). The trimming parameters of raw sequences were determined with figaro v1.1.2 (Sasadaet al., 2020). DADA2 v1.21.0 was used for quality filtering, error rate learning, sample inference, redundancy removal (duplicate sequences), paired read merging, amplicon sequence variant (ASV) table construction, and

chimera removal(Callahanet al., 2016). Taxonomy classification based on SILVA138.1 (Quastet al., 2013) and phylogenetic reconstruction were conducted using QIIME2 2020.11 (Bolyenet al., 2019). The sequencing data have been deposited in the NCBI database, with reference code PRJNA907956.

Each sample was rarefied to 14,587 sequences for comparison. For quality control, the ASVs detected less than 3 times (once and twice) were removed from further analysis (Guoet al., 2022). The core ASVs were defined by the threshold of occurrence (>60 %) and relative abundances (>0.1 %). The alpha diversity was determined using the Chao1 and Shannon indices. Principal coordinates analysis (PCoA) was performed based on both weighted and unweighted UniFrac metrics. The linear discriminant analysis effect size (LEfSe) was applied to determine the key sensitive ASVs that were significantly influenced by selected factors (significance threshold > 4). Permutational multivariate analysis of variance (PERMANOVA) was used to test and determine the significance ($p < 0.05$) (Anderson and Walsh, 2013). Adonis analysis that employs weighted UniFrac metrics was used to decompose the total variance and analyze the explanatory degree of different grouping factors to sample differences. PERMANOVA/Adonis analysis was conducted using the vegan R package (Dixon, 2003).

### 2.7. Network analyses

The remaining 1,674 ASVs for biofilm and 852 ASVs for water were used for network construction. To measure community-wide species co-occurrence patterns and microbial community assembly rules, the checkerboard score (C-score), which examines actual species distributions, was used (Barberánet al., 2012; Fayleet al., 2013). It calculates the number of 2 × 2 species matrices, where both species occur only once but at different sites and compares the real data with a random simulated score under the null model (Stone and Roberts, 1990). The C-score and its variance ($C_{var}$-score) tests were conducted using the oecosimu function in the R vegan package with the sequential swap randomization algorithm and 30,000 simulations (Dixon, 2003).

To explore co-occurrence associations in different sample types and groups, corresponding correlation matrices were constructed by all possible pairwise Spearman rank coefficients (ρ). Only robust ($\rho \geq 0.6$) and statistically significant ($p < 0.01$) correlations were used for network construction (Barberánet al., 2012). Network visualization and modular analysis were performed using Gephi 0.9.2, in which 10,000 Erdös-Réyni random networks with the same number of nodes and edges as the empirical networks were generated (Juet al., 2014). Topological properties, including the clustering coefficient (CC), modularity (MD), average shortest path length (APL), network diameter (ND), average degree (AD), and small-world coefficient (σ), were calculated and compared for both empirical and random networks (Telesfordet al., 2011). The connectivity of the ASV (node) reveals its topological roles in the network. According to within-module connectivity (Zi) and among-module connectivity (Pi), nodes were divided into 4 categories: (i) peripheral nodes (specialists, $Zi \leq 2.5$, $Pi \leq 0.62$); (ii) connectors (generalists, $Zi \leq 2.5$, $Pi > 0.62$); (iii) module hubs (generalists, $Zi > 2.5$, $Pi \leq 0.62$); and (iv) network hubs (supergeneralists, $Zi > 2.5$, $Pi > 0.62$) (Guimerà and Nunes Amaral, 2005; Olesenet al., 2007). Typically, the connectors, module hubs, network hubs are classified as key nodes (i.e., keystone ASV) (Denget al., 2012). All analyses were performed with the R packages vegan, igraph and Hmisc.

## 3. Results

### 3.1. Composition and diversity of bacterial communities

An overview of the obtained sequences, sequences after rarefying, number of ASVs after rarefying, number of ASVs after filtering out rare instances, and number of cores ASVs are summarized in Table S5. In total, 14,433,833 raw sequences were obtained from 178 samples (81 water, 97 biofilms, 14,587–111,559 sequences/sample), which were assigned to 15,084 ASVs. The rarefaction curves eventually plateaued, suggesting that sufficient sample coverage was achieved in this study (Fig. S2). After rarefaction to the lowest sequencing depth (14,587), 2,596,486 sequences were obtained, which were assigned to 12,262 ASVs. Removing the ones detected less than 3 times (once and twice), there remained 2,513,842 sequences and 1,798 ASVs. The number of observed ASVs in biofilms was much higher than that in water (1674 vs. 852). As shown in Fig. 1A, there were 728/1,798 ASVs shared by biofilm and water, which accounted for 90.7 % of the total sequences. Although the number of biofilm-specific ASVs was high (946/1,798, 52.6 %), they accounted for only 8.7 % of the total sequences. Compared to biofilm, both the number (124/1,798) and abundance (0.7 %) of water-specific ASVs were much lower. The abundance-occupancy relationship is shown in Fig. 1B. Thirty-three ASVs were identified as core ASVs (occupancy > 60 %, relative abundance > 0.1 %), which covered 72.8 % of the total sequences. The 12/33 core ASVs shared by water and biofilm accounted for 62.2 % of the total sequences. The details of the core ASV ID and taxonomy information are shown in Table S6.

At the phylum level, all samples were dominated by Proteobacteria (50.5–99.9 %) regardless of sampling location and type. As shown in Fig. 2, the bacterial communities of biofilm were dominated by Alphaproteobacteria (62.8 ± 28.4 %), Gammaproteobacteria (20.5 ± 30.6 %), and Actinobacteria (6.8 ± 6.4 %), while planktonic bacteria in water were predominated by Alphaproteobacteria (95.9 ± 6.8 %). At the genus level, *Phreatobacter* spp. (shared core, ASV1) was dominant in both biofilm (29.5 ± 28.3 %) and water (22.0 ± 15.2 %) (Figure S3, Table S7). An unclassified genus belonging to the f_Sphingomonadaceae (shared core, ASV2) was dominant in water (17.2 ± 12.7 %) and biofilm (7.8 % ± 16.4). In addition, within the community of planktonic bacteria, nine out of the top ten ASVs belonged to f_Sphingomonadaceae (e.g., g_*DSSF69*, g_*Sphingorhabdus*, g_*Porphyrobacter*, g_*Novosphingobium*), the summed relative abundances of which accounted for 60.5 %.

The total bacterial gene copies in biofilm and water were $1.0 \times 10^4$ to $3.4 \times 10^6$ gene copies/cm$^2$ and $2.8 \times 10^3$ to $6.6 \times 10^4$ copies/mL. For biofilm samples, the mean arithmetic values of total bacterial gene copies in S-Zn (SL), S-Zn (PP) and S-PE (SL) pipes (Figure S4) were $5.0 \pm 7.8 \times 10^5$ gene copies/cm$^2$, $9.8 \pm 7.4 \times 10^5$ gene copies/cm$^2$ and $2.0 \pm 2.0 \times 10^5$ gene copies/cm$^2$, respectively.

The PCoA based on weighted UniFrac metrics showed that the water samples were more congregated, while biofilm samples were more dispersed (Figure S5), indicating that the bacterial communities in the water samples were similar to each other, while the bacterial communities varied among the biofilm samples (betadisper, $F = 85.475$, $p < 0.001$). Statistically, although they might be affected by nonhomogeneous dispersion of the data, the PERMANOVA results revealed significant differences in beta diversity between the water and biofilm samples (adonis, $F = 23.217$, $p = 0.001$). The distance between biofilm samples is greater than the distance between biofilm samples and water samples (Figure S6). Spatially, for the locations where both water and biofilms were sampled (L1-L8), it is clear that compared to the PCoA based on weighted UniFrac metrics (adonis, $F = 7.088$, $p = 0.001$) (Fig. 3A), the PCoA based on unweighted UniFrac metrics showed that water and biofilm were clearly in different clusters, indicating clear differences in memberships of the bacterial communities of water and biofilm (adonis, $F = 11.875$, $p = 0.001$) (Fig. 3B). The differences between results based on weighted and unweighted UniFrac metrics suggested that the highly abundant ASVs are similar in the water and biofilm.

### 3.2. Key influencing factors

**Pipe ages.** When grouped by age (e.g., 10–20 years, n = 8; 20–30 years, n = 24; 30–40 years, n = 32; 40–50 years, n = 8), the Chao1 index was significantly higher for 40–50 years than for 10–20 years ($p < 0.05$) (Fig. 4A), while Shannon diversity significantly higher for 40–50 years

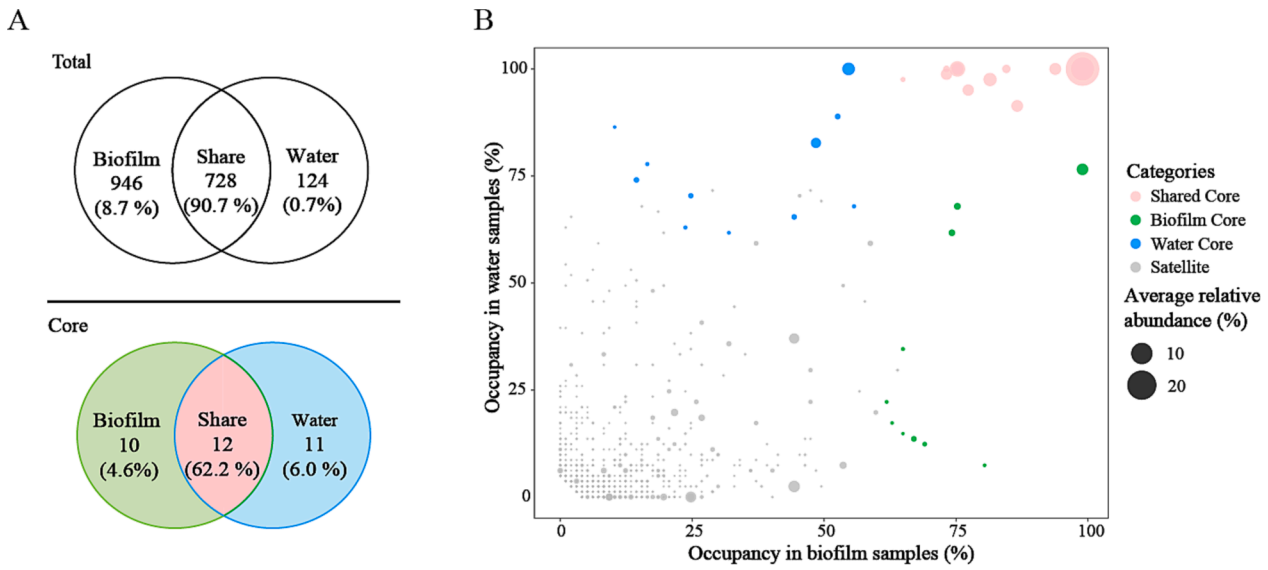


**Fig. 1.** The total, core and shared ASVs in water and biofilm across all locations: (A) Venn diagram showing the number of ASVs and relative abundances of each category; (B) Bubble diagram showing occupancy-abundance plot of ASVs in the 97 biofilm (x-axis) and 81 water (y-axis) samples (core ASVs: occupancy > 60 %; relative abundance > 0.1 %). The size of circles was proportional to the average relative abundance of the corresponding ASVs.

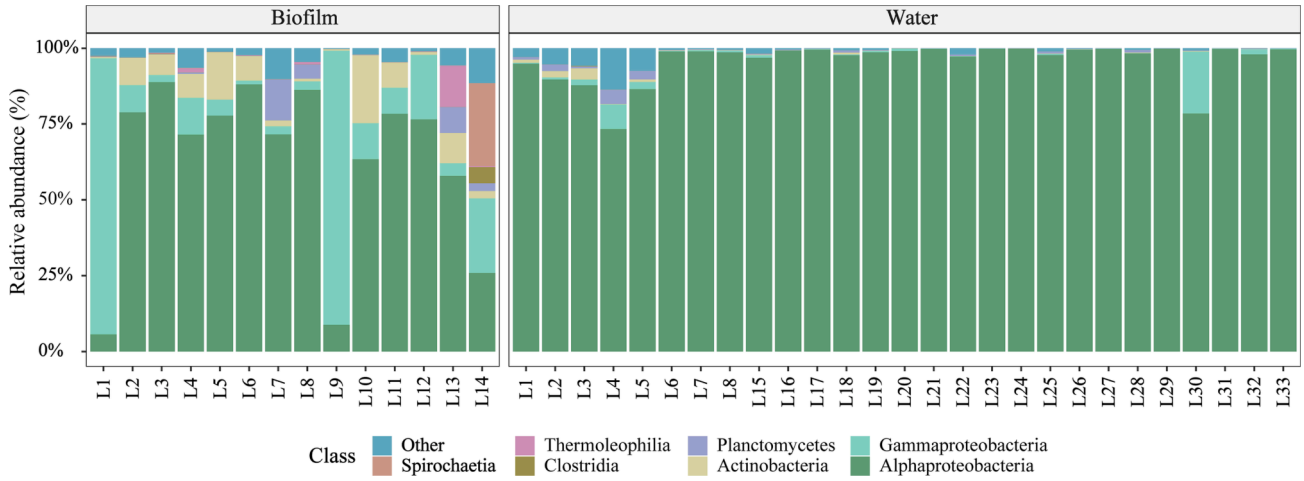


**Fig. 2.** The bacterial community composition of biofilm and water samples at the class level. The classes with relative abundance > 5 % are presented, the rest of classes are grouped as others. For biofilm samples, n = 97; for each location, n = 8 for L1-L6 and L9-L13, n = 3 for L7, L8, and L14. For water samples, n = 81; for each location, n = 3.

than 10–20 and 20–30 years, but remained similar at 10–20 years to 20–30 years (Fig. 4B). The sharing of ASVs among age groups is shown in a Venn diagram (Figure S7A), and ASVs sensitively influenced by pipe ages were determined by LEfSe (Figure S8A, Table S8). The relative abundance of ASV2 (f_Sphingomonadaceae) was lower for pipe ages 40–50 years (7.9 %) than for pipe ages 10–20 years (59.3 %), while ASV14 (f_Sphingomonadaceae), ASV8 (f_Hyphomonadaceae), and ASV10 (f_Hyphomonadaceae) increased to 5.3 %, 6.6 %, and 19.5 % at 40–50 years after their presence at 20–30 years. Interestingly, ASV26 (g_*Mycobacterium*) was dominant in the 10–20 years biofilm, ASV9 (g_*Acidovorax*, 11.9 %) was dominant in the 20–30 years biofilm, and ASV13 (g_*Pseudomonas,* 8.6 %), ASV24 (f_Hyphomonadaceae, 2.1 %), ASV17 (g_*Sphingorhbdus*, 2.2 %), ASV20 (g_*Pseudomonas*, 3.0 %), and ASV23 (g_*Paryiterrbacter*, 2.7 %) were dominant in the 30–40 years biofilm, all of which were hardly detected in the other age groups. The PCoA plot of biofilms among age groups is shown in Figure S9A. Although not clearly separated into different clusters, the PERMANOVA results showed that pipe age had a significant influence on the bacterial community of biofilms (adonis, F = 8.944, $p$ = 0.001). Moreover, the dispersion of bacterial communities differed significantly among age groups (betadisper, F = 5.543, $p$ = 0.001), for which the 10–20 years and 40–50 years biofilms appeared to be less dispersed, while the 20–30 years and 30–40 years biofilms were more dispersed.

**Pipe types.** The pipe ages were not significantly different between the groups of pipe type and materials. For S-Zn pipes, with grouping by the types of pipes (service line, SL, n = 72; premise plumbing, PP, n = 6), it was observed that the Chao1 (Fig. 4D, $p < 0.05$) and Shannon index (Fig. 4E, $p < 0.001$) values of biofilm on PP were significantly higher with respect to biofilm on SL. The type of pipes showed significant influences on the bacterial community of biofilms (adonis, F = 10.041, $p$ = 0.001; betadisper, F = 1.4073, $p$ = 0.2392) (Figure S9B). As shown in Fig. 4F and Figure S8B, premise plumbing has higher relative abundances with ASV14 (f_Sphingomonadaceae), ASV17 (g_*Sphingorhabdus*), ASV50 (g_*Amphiplicatus*), ASV38 (f_Rhodobacteraceae), ASV32 (f_Sphingomonadaceae) and ASV43 (g_*Sphingopyxis*) and less relative abundances with ASV1 (g_*Phreatobacter*), ASV2 (f_Sphingomonadaceae),

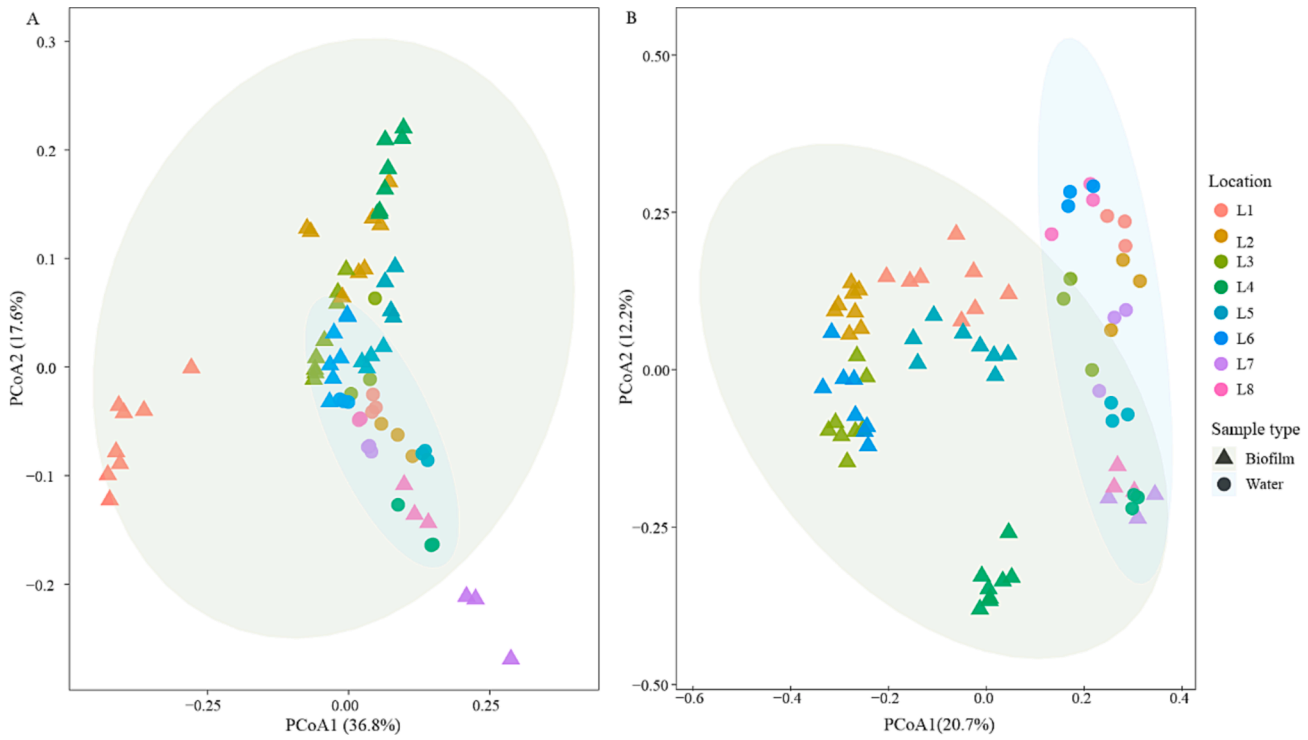


**Fig. 3.** The bacterial community similarity between water and biofilm. PCoA plot for the locations (L1-L8) with paired water and biofilm samples based on (A) weighted UniFrac; (B) unweighted UniFrac metrics. The colored ellipses represent to 95% confidence intervals.

ASV7 (g_*Rhodococcus*), ASV9 (g_*Acidovorax*), and ASV10 (f_Hyphomonadaceae) than service lines, detailed information was shown in Table S9.

**Pipe material.** For the service lines, biofilms were sampled from S-Zn (n = 72) and S-PE pipes (n = 19). The Chao1 index (Fig. 4G, $p < 0.05$) and Shannon diversity (Fig. 4H, $p < 0.05$) of biofilms on S-PE were higher than those on S-Zn. As shown in Figure S9C and confirmed by PERMANOVA tests, pipe material had a significant influence on the bacterial communities of biofilms (adonis, F = 10.359, $p = 0.001$; betadisper, F = 0.9707, $p = 0.3272$). As shown in Fig. 4I and Figure S8C, S-Zn pipes were enriched in ASV10 (f_Hyphomonadaceae), ASV13 (g_*Pseudomonas*), and ASV2 (f_Sphingomonadaceae), while S-PE was enriched in ASV5 (f_Sphingomonadaceae), ASV27 (g_*Mycobacterium*), ASV37 (f_Spirochaetaceae), ASV17 (g_*Sphingorhabdus*), and ASV23 (g_*Parviterribacter*), detailed information was shown in Table S10.

**Water quality.** RDA confirmed that the first and second axes explained 67.0 % of the cumulative variances in the biofilm and water core ASVs and environmental factors (Fig. 5). As shown by RDA, $NO_3^-$, Ca, Al, pipe age and residual chlorine exerted significant effects on core ASVs ($p < 0.001$), which revealed a clear positive correlation between pipe age and $NO_3^-$. Moreover, there was a strong association between microbial ASVs and environmental factors: 1) ASV1 (g_*Phreatobacter*) and Al; 2) ASV2 (f_Sphingomonadaceae) and residual chlorine-Al; 3) ASV3 (g_*DSSF69*), ASV6 (g_*DSSF69*) and residual chlorine; 4) ASV7 (g_*Rhodococcus*) and Al; 5) ASV4 (g_*Sphingorhabdus*), ASV8 (f_Hyphomonadaceae), ASV10 (f_Hyphomonadaceae), ASV24 (f_Hyphomonadaceae) and age-$NO_3^-$; 6) ASV4 (g_*Sphingorhabdus*), ASV11 (g_*Sphingorhabdus*), ASV12 (f_Porphyrobacter), ASV14 (f_Sphingomonadaceae) and Ca.

### 3.3. Co-occurrence patterns and bacterial community assembly

**Nonrandom assembly.** The observed C-scores (BF: 46.1, WA: 25.0) were significantly higher than the simulated mean values under the null model (BF: 42.7, WA: 21.6; $p < 0.0001$), indicating the segregated species distributions of bacteria in water and biofilm (Fig. S10). Similarly, the same trends of $C_{var}$ scores revealed greater degrees of species aggregation (i.e., positive interactions) and segregation (i.e., negative interactions) than expected (Table S11). Combining C-score and $C_{var}$-score tests, it can be concluded that the assembly patterns of bacteria in service lines and premise plumbing were nonrandom, while the larger $C_{var}$-score standardized effect size (SES) values for biofilm than water suggested stronger strength of species aggregation and segregation, which may be attributed to the highly heterogeneous structure and microenvironments within biofilm.

**Co-occurrence networks.** The topological properties of the co-occurrence networks of biofilm and water are given in Table 2. The numbers of nodes (ASVs) and edges (connections) of biofilm were higher than those of water, while the cluster coefficients, modularity and average shortest path lengths in both water and biofilm were much higher than for their identically sized Erdös-Réyni random networks. The small-world coefficient ($\sigma > 1$) and modular structures (MD > 0.4) indicated that both networks had "small-world" properties (i.e., high interconnectivity and efficiency). The higher cluster coefficients and average degree, together with lower APL and network diameter in the water network compared to the biofilm network, suggested that the planktonic bacteria are more closely connected to each other, facilitating rapid information transfer.

Bacterial co-occurrence networks for water and biofilm are visualized and colored in Fig. 6. For both water and biofilm, the significantly co-occurring ASVs mostly belonged to Proteobacteria (44.5 % and 52.8 %), Planctomycetota (16.5 % and 15.9 %), Actinobacteriota (12.1 % and 7.8 %) and Acidobacteriota (5.8 % and 4.7 %) (Fig. 6A and 6C).

The modularity of the biofilm network is lower than that of the water network (Table 2). As shown in Fig. 6B and 6D, the water network was mainly composed of four visually distinct modules linked with a few points, while there were more connections between modules in the biofilm network. When integrating module and taxonomic data, it was found that taxonomic relatedness is a key factor determining network modular structure, e.g., the ASV-ASV co-occurrence of Proteobacteria

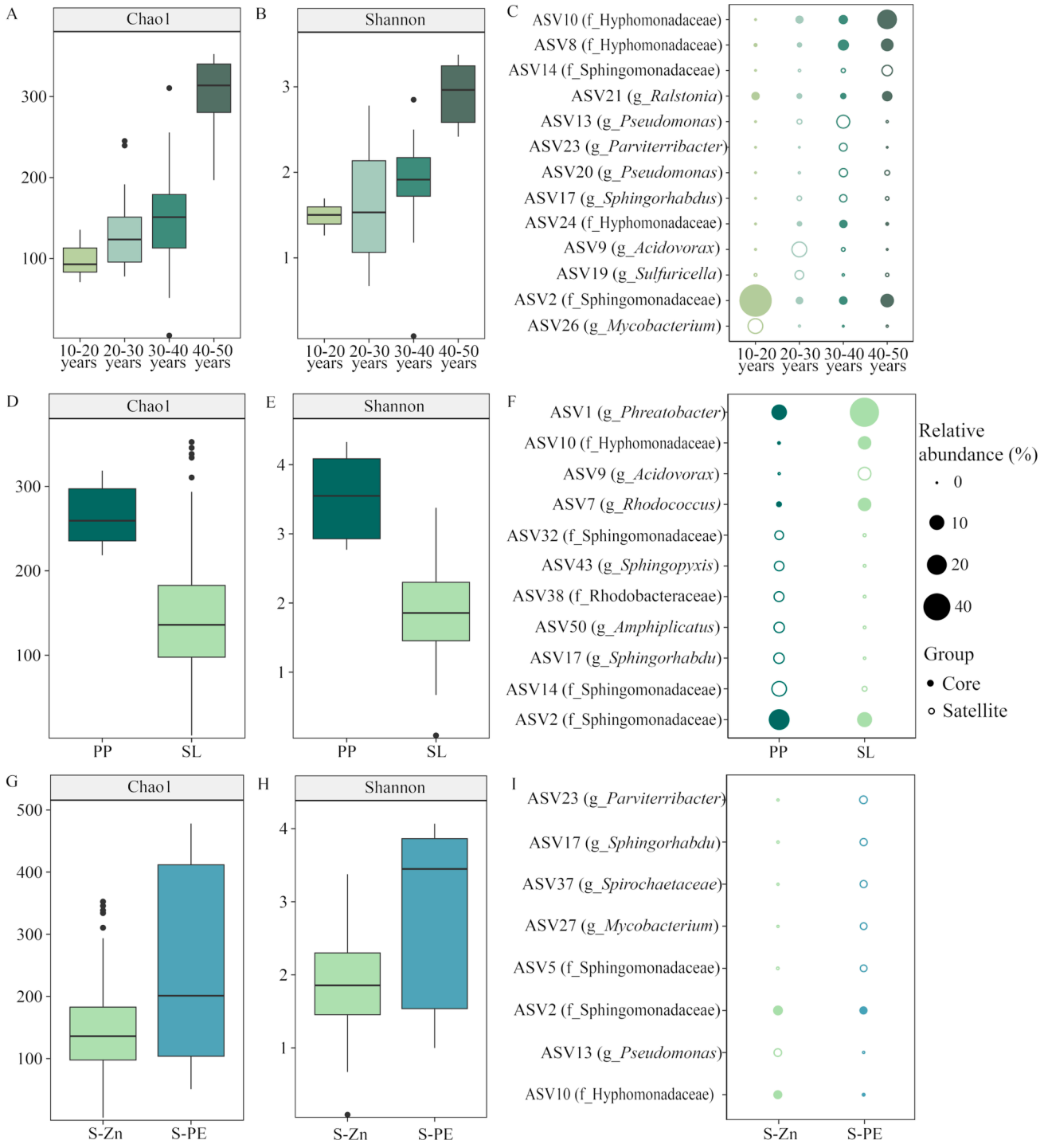


**Fig. 4.** The influences of pipe ages (10–20 years (n = 8), 20–30 years (n = 24), 30–40 years (n = 32) and 40–50 years (n = 8) years, all service line, S-Zn pipes), pipe types (service line, SL (n = 72); premise plumbing, PP (n = 6); S-Zn pipes), and pipe material (S-Zn (n = 72), S-PE (n = 19); service line) on the Chao1 index, Simpson diversity and enriched ASVs of biofilm bacterial communities and: (A) influence of pipe ages on Chao1 index; (B) influence of pipe ages on Shannon diversity, (C) relative abundances of sensitive ASVs enriched by different pipe ages; (D) influence of pipe types on Chao1 index; (E) influence of pipe types on Shannon diversity; (F) relative abundances of sensitive ASVs enriched by different pipe types; (G) influence of pipe material on Chao1 index; (H) influence of pipe material on Shannon index; (I) relative abundances of sensitive ASVs enriched by different pipe material.

and Planctomycetota within module 1. In addition, biotic interactions, ecological niches, and environmental filtering may be additional drivers of strong bacterial co-occurrences, e.g., module 8 in the water network and module 5 in the biofilm network. Remarkably, the great majority of core ASVs (occupancy > 60 %, relative abundance > 0.1 %) were at the edge of the network, which had a small degree and few connections with satellite ASVs (Fig. S11A and 11B). Most ASVs in both biofilm (99.4 %) and water (99.6 %) were peripherals with links to ASVs within modules. Regarding the keystone ASVs, ASV97 (g_*Pirellula*) and ASV739 (g_*Hyphomicrobium*) were identified as module hubs in the water networks and ASV419 (f_Beijerinckiaceae), ASV632 (o_Candidatus_Yanofskybacteria), ASV801 (c_KD4-96), ASV925 (f_67-14) and ASV960 (g_*Gaiella*) were identified as module hubs in biofilm networks (Table S12), all of which had inside-module connections. All identified

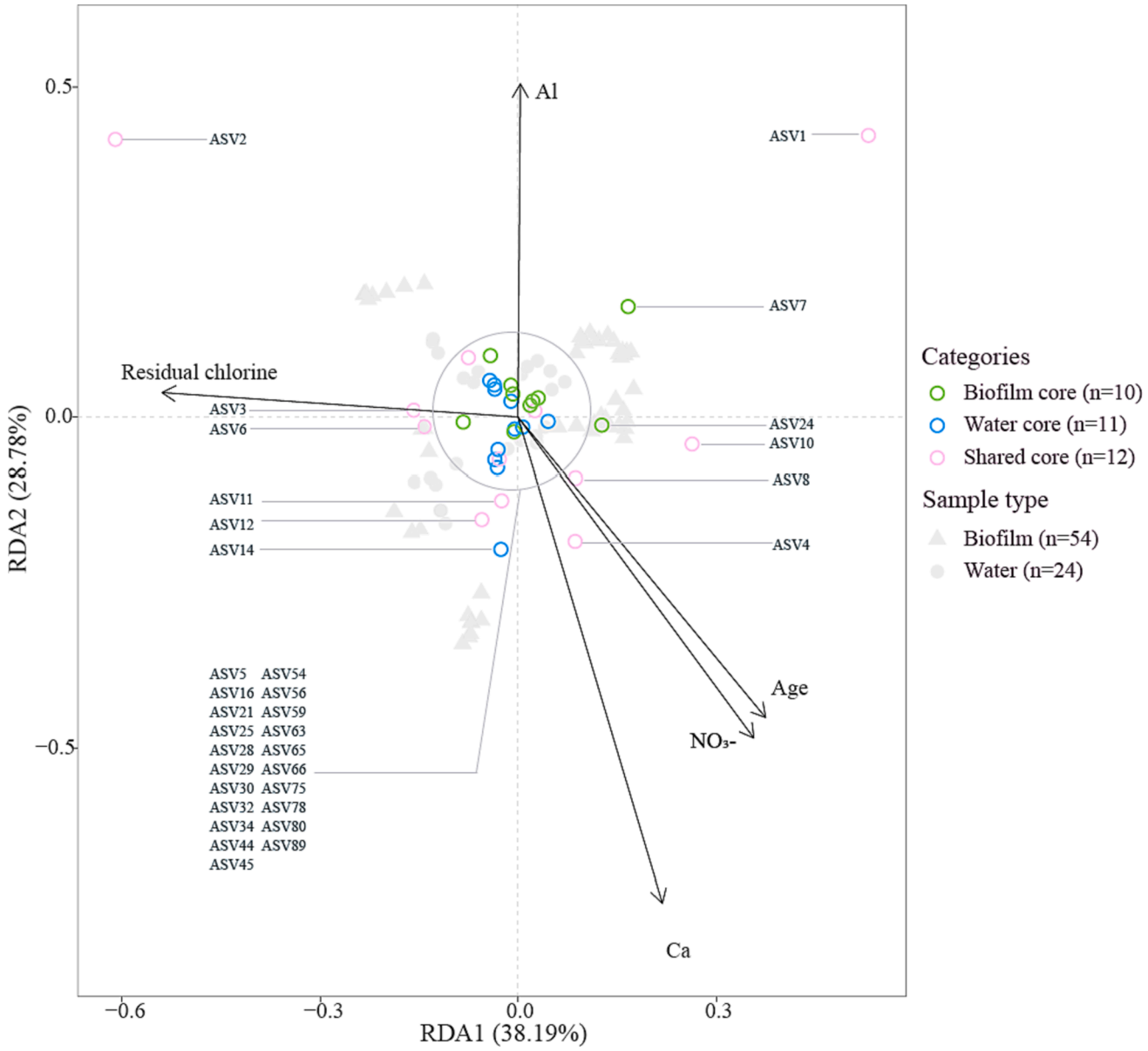


**Fig. 5.** RDA ordination plot of the relationship between environmental factors and detected core ASVs.

**Table 2**
Topological properties of the empirical co-occurrence networks of biofilm and water bacterial communities and an associated random work.

| Objects | | Nodes | Edges | Clustering coefficient (CC) | Modularity (MD) | Average shortest path length (APL) | Network diameter (ND) | Average degree (AD) | Small-world coefficient (σ) |
|---|---|---|---|---|---|---|---|---|---|
| Biofilm | Empirical | 878 | 16,734 | 0.799 | 0.327 | 3.044 | 12 | 38.118 | 26.443 |
| | Random | | | 0.043 ± 0.001 | 0.099 ± 0.002 | 2.139 ± 0.001 | 3 | 38.118 | |
| Water | Empirical | 511 | 5,468 | 0.794 | 0.419 | 4.109 | 19 | 21.401 | 9.321 |
| | Random | | | 0.042 ± 0.001 | 0.153 ± 0.005 | 2.026 ± 0.002 | 4 | 21.401 | |

***Abbreviations:*** *Small-word coefficient $\sigma = (CC/CCr)/(APL/APLr)$, where $\sigma > 1$ suggests 'small-world' properties. Subscript r indicates the properties of the identically sized Erdös-Réyni random network.*

key ASVs are satellites rather than cores, suggesting that low abundance members may play key roles in the service lines and premise plumbing bacterial communities (Fig. S12).

## 4. Discussion

### 4.1. Communities of planktonic bacteria and biofilm

In this study, the diverse and complex communities of both planktonic bacteria and biofilm were dominated by Proteobacteria, which concurs with previous drinking water system studies regardless of the differences in geography, treatment processes, and disinfectants applied

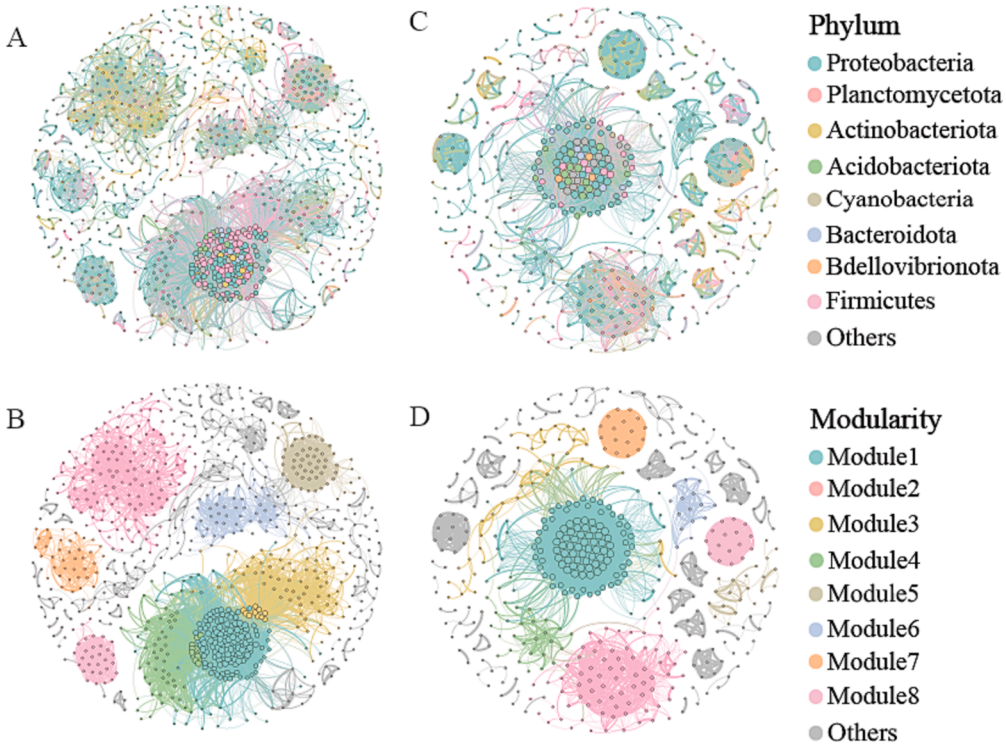


**Fig. 6.** Co-occurrence networks of biofilm (A-B) and water (C-D) bacterial communities based on correlation analysis. Nodes indicating ASVs (appearing in at least 3 samples) are colored by phylum (A and C) and modularity class (B and D), and the size is proportional to degree. Edges represent robust ($\rho \geq 0.6$) and statistically significant ($p < 0.01$) correlations, and the edge thickness of each connection between two nodes (weight) is proportional to the correlation coefficient. The "edge thickness" refers to the thickness of the line connected between two nodes. The higher the correlation between two nodes, the thicker the line.

(Proctor and Hammes, 2015). The predomination of Alphaproteobacteria in planktonic bacteria (>95 %), and higher relative abundances of Gammaproteobacteria (20.5 %) and Actinobacteria (6.8 %) in biofilms than water were also reported previously in chlorinated drinking water systems (Panet al., 2021; Wuet al., 2015). Interestingly, both planktonic bacteria and biofilm were dominated by ASV1 (g_*Phreatobacter*) and ASV2 (f_Sphingomonadaceae), the sum relative abundances of which accounted for 39.2 % in planktonic bacteria and 40.8 % in biofilm. The presence and domination of g_*Phreatobacter* in planktonic bacteria and biofilms have been reported in other studies in the distribution systems of Beijing (16.7–26.5 %) and Paris (4.5–23.7 %) (Jinget al., 2021; Perrinet al., 2019). In addition, the detection of f_Sphingomonadaceae in planktonic bacteria and g_*Pseudomonas* and g_*Rhodococcus* in biofilms was also consistent with previous observations (Doutereloet al., 2017; Martinyet al., 2005; Tanget al., 2021; Zhanget al., 2022).

Comparing planktonic bacteria and biofilms, most of the ASVs in water were also present in biofilms (728/852, 85.4 %), while only 43.5 % of ASVs in biofilms (728/1,674) were present in water. In other words, the communities of biofilms were more diverse than those of planktonic bacteria, which was reported previously and may be caused by the multiple microenvironments within biofilms allowing the proliferation of different bacteria (Doutereloet al., 2013; Henneet al., 2012). Moreover, since water is considered a seed bank for biofilm communities (Henneet al., 2012), the acquired water samples were only snapshots, while biofilm samples were subjected to accumulative impacts of feed water, pipe age, pipe material and local circumstances. This might be precisely the reason for the highly similar planktonic communities and significantly different biofilm communities within the studied distribution area. In contrast, previous studies in the Dutch system observed highly similar biofilm communities across distribution systems, which may be attributed to the smaller unchlorinated system and the fact that the same pipe material and pipe ages were studied (Liuet al., 2014; Liuet al., 2018).

Service lines have longer stagnation time and lower disinfectant concentrations than distribution main pipe, favoring microbial interactions between water and biofilms. A previous study has confirmed service lines contributed more than mains to the particulate material at customer taps (57.6 ± 13.2 % vs 13.0 ± 11.6 %), and the biofilm samples from mains and water were grouped into two separate clusters, the cluster of biofilms on service line fell between the biofilms on main pipes and water (Fanget al., 2023). Similarly, in our study, the community compositions of the paired water and biofilm samples were significantly different ($p = 0.001$) though did not visually form two distinct clusters.

### 4.2. *Key influencing factors for bacterial communities of biofilms*

In this study, the results revealed different but significant influences of pipe age, pipe type, and pipe material on the bacterial communities of biofilms. For pipe age (10–20 years, n = 8; 20–30 years, n = 24; 30–40 years, n = 32; 40–50 years, n = 8), as observed via Chao1 and Shannon diversity (Fig. 4), the species richness and diversity of biofilm correlates with pipe age (10–20 to 40–50 years), which means that the biofilm continued to evolve and develop regarding the community composition and diversity even after decades of service. This is different from one previous pilot study that suggested that biofilm in a water distribution system reached a steady state in one to three years (~500 days) (Martinyet al., 2003). The possible reason for this might be that the longest pilot study was three years (Boe-Hansenet al., 2002; Manuelet al., 2007; Martinyet al., 2003), while in the real world, the building up of biofilms may establish internal recycling of resources and create multiple micro-niches for increased species richness and diversity over time (Jacksonet al., 2001). The results of this study are realistic illustrations of lifetime biofilm succession, assuming a service line service time of 50 years. However, it should be noticed that different from sequentially sampling over years from similar point or same reactor, this study sampled biofilm with different ages from different locations in

real-world distribution system. The sequential sampling over years in real-world distribution system would be hardly possible because of the difficulties in digging, cutting and maintaining distribution pipes. Whereas, when exploring results of the present study, the potential influences of locations and/or other conditions should be kept in mind.

Regarding the influences of pipe types (all galvanized steel pipes), it was found that the biofilm communities harbored by premise plumbing (n = 6) had significantly higher species richness and diversity than those of the service line (n = 72). This agrees with a previous study in an unchlorinated system, where the household connection pipes harbored three times more species than the service line pipes (Liuet al., 2017a). Similarly, Huang et al. found that the Shannon diversity of premise plumbing biofilm samples was higher than outdoor biofilm in a looped and continuous plumbing, which was attributed to high and stable indoor temperature (Huanget al., 2021). Factors such as higher temperature, longer residence time, more stagnant periods, and larger surface to volume ratio in premise plumbing than in service lines almost entirely favor bacterial growth (Linget al., 2018; Neu and Hammes, 2020; Wanget al., 2017). Quantitatively, we observe higher biomass in premise plumbing ($9.8 \pm 7.4 \times 10^5$ gene copies/$cm^2$) than in service lines ($5.0 \pm 7.8 \times 10^5$ gene copies/$cm^2$). For the megacity of Beijing, the premise plumbing would have more significant influences on biofilm and customer tap microbiology since it is very common to have apartment buildings between 20 and 30 floors. Considering that premise plumbing is a hotspot for (opportunistic) pathogens (De Sottoet al., 2020; Falkinhamet al., 2015; Rhoadset al., 2017; Wanget al., 2017), microbial risk assessment and management for ultra large premise plumbing within megacities deserves more attention.

In addition, this study found that the biofilm community of S-PE pipes (service line, n = 19) had higher species richness and diversity than that of S-Zn pipes (service line, n = 72). This complies with a previous simulated study of biofilms in reclaimed water distribution systems for one year (high throughput sequencing), which attributed the low species richness and diversity to the toxicity of Zn (Zhanget al., 2019). A previous study discovered that low concentrations of $Zn^{2+}$ inhibited splicing mediated both by the RecA intein from *Mycobacterium tuberculosis* and the inhibition of $Zn^{2+}$ may be a relatively general phenomenon (Mills and Paulus, 2001). In contrast, an earlier short-term (90 days) batch study (Denaturing gradient gel electrophoresis (DGGE) band sequencing) reported similar species richness and diversity between biofilms of S-PE and S-Zn pipes (Yuet al., 2010). The different findings from Yu et al. may either be due to short biofilm age or DGGE analysis, which only represent a few numerically dominant phylotypes. Coincidentally, in both abovementioned studies, the quantity of biofilm (ATP/$cm^2$, cells/$cm^2$) of S-Zn pipes was much higher than that of S-PE pipes, indicating that the low species richness and diversity were not caused by the general toxicity of Zn to bacteria. It is likely that Zn can selectively inhibit and/or promote bacterial growth. 2-Aminoimidazoles chelate Zn promote inhibit *Mycobacterium abscessus* biofilms growth (Belardinelliet al., 2022). In addition, previous study found that the minimum inhibitory concentrations (MICs) of zinc nanoparticles (60 nm) to *Mycobacterium tuberculosis*, *Escherichia coli* and *Pseudomonas aeruginosa* were 1.25 mg/mL, 10 mg/mL, > 10 mg/mL, respectively (Punjabiet al., 2018). Ren et al. found that g_*Pseudomonas* (43.33 %) were predominant in the biofilm from galvanized steel pipe(Renet al., 2015). In this study, ASV27 (g_*Mycobacterium*) was dominant in S-PE biofilms but absent in S-Zn biofilms, and ASV13 (g_*Pseudomonas*) was enriched in S-Zn biofilms. Further research is needed and recommended to understand the specific mechanism. Overall, the complex succession and evolution of biofilms in field drinking water distribution are simultaneously influenced by factors such as pipe age, pipe type, pipe material, temperature, disinfectant, water age, water chemistry and hydraulic conditions (Daiet al., 2020; Learbuchet al., 2021; Lehtolaet al., 2004; Liet al., 2020; Proctoret al., 2017; Wanget al., 2014). The combination of these factors rather than any single factor shapes the biofilm community. Therefore, although this study sheds new light on real-world biofilm evolution, it is difficult to separate the effect of each parameter. It should be noted that the sample sizes are different among the compared groups. Ideally, the sample size of each category/group should be kept the same, however, because of the difficulties in obtaining real-world biofilm samples, it is common to have different sample sizes for comparison (Potgieteret al., 2018; Proctoret al., 2018). Therefore, though there might be limitations due to different sample sizes, statistically, it would be reasonable and reliable to have such comparison and draw the conclusions.

### 4.3. Low-abundance members maybe key players in biofilm community

In this study, five rare ASVs were identified as module hubs in the biofilm network (Figure S12; Table S12). Although these five ASVs were rare members with low abundance (<0.1 %), they were keystone ASVs for intramodular connections in the BF network. Previously, rare members were identified as keystone species in biofilms of anaerobic digestion reactors, membrane bioreactors, and microbial electrolysis cells (Fenget al., 2017; Guoet al., 2022; Xuet al., 2019). It is interesting to observe that keystone ASVs were present and had high relative abundances in the oldest biofilm on S-Zn pipes (45 years), indicating possible higher stability and resilience of the older biofilm community (Guoet al., 2022). Rare species in drinking water have attracted considerable attention, mainly for opportunistic pathogens for biosafety reasons, such as *Legionella pneumophila*, *Pseudomonas aeruginosa* and *Mycobacterium avium* (Dowdellet al., 2019; Nortonet al., 2004; Vaerewijcket al., 2005; van der Kooijet al., 2017; Wanget al., 2012). However, studies regarding the bacterial community and microbial ecology within distribution systems are still limited to dominant species. As observed in the present study, the rare but keystone ASVs were either module and network hubs or connectors in the community, which may play key roles in maintaining function and stability of biofilm community. This agrees with previous findings that rare species pulls ecosystems strings, and involves in important microbial driven processes such as nutrient cycling, pollutant degradation, host health and community assembly (Joussetet al., 2017). Therefore, rare species would deserve more research attention in the future studies of biofilms in drinking water systems.

## 5. Conclusion

In summary, this study comprehensively assessed the communities of planktonic bacteria and biofilm in the field drinking water distribution system of a megacity, with a special focus on the service lines and premise plumbing. The pipe ages, material and types have significant influences on the communities of real-world biofilm. The following conclusions can be drawn:

- The community of both planktonic bacteria and biofilm were dominated by Proteobacteria. The 33 core ASVs covered 72.8 %, while the 12 shared core ASVs accounted for 62.2 % of the total sequences.
- For pipe age (10–20 years, n = 8; 20–30 years, n = 24; 30–40 years, n = 32; 40–50 years, n = 8), the species richness and diversity of biofilm communities positively correlates with pipe age. The relative abundance of ASV2 (f_Sphingomonadaceae) was lower for pipe ages 40–50 years (7.9 %) than for pipe ages 10–20 years (59.3 %), while the relative abundance of ASV10 (f_Hyphomonadaceae) was higher for pipe ages 40–50 years (19.5 %) than its presence at pipe ages 20–30 years (1.9 %).
- For pipe type, the community of the premise plumbing biofilm (n = 6) had significantly higher species richness and diversity than the service line biofilm (n = 12). Compared to the service line, premise plumbing selectively promoted the growth of certain members, e.g., ASV17 (g_*Sphingorhabdus*), ASV50 (g_*Amphiplicatus*), and ASV43 (g_*Sphingopyxis*).

- For pipe material, S-PE (n = 19) harbored a significantly more diverse biofilm community than S-Zn (n = 72), bacterial communities of biofilms had a significant different between S-PE and S-Zn, while both clearly enriched different ASVs: e.g., S-PE enriched ASV27 (g_*Mycobacterium*) and S-Zn enriched ASV13 (g_*Pseudomonas*).
- Not core ASVs, but five rare ASVs, were identified as keystone members, indicating the potential importance of rare members in mature biofilm communities.

## CRediT authorship contribution statement

**Anran Ren:** Writing – original draft, Software, Methodology. **Mingchen Yao:** Software. **Jiaxing Fang:** Software. **Zihan Dai:** Software. **Xiaoming Li:** Writing – review & editing, Methodology. **Walter van der Meer:** Resources. **Gertjan Medema:** Supervision. **Joan B. Rose:** . **Gang Liu:** Writing – review & editing, Supervision.

## Declaration of competing interest

The authors declare that they have no known competing financial interests or personal relationships that could have appeared to influence the work reported in this paper.

## Data availability

Data will be made available on request.

## Acknowledgments

The present work has been financially supported by the National Natural Science Foundation of China (52022103).

## Appendix A. Supplementary data

Supplementary data to this article can be found online at https://doi.org/10.1016/j.envint.2024.108538.

## References

Aggarwal, S., Gomez-Smith, C.K., Jeon, Y., LaPara, T.M., Waak, M.B., Hozalski, R.M., 2018. Effects of chloramine and coupon material on biofilm abundance and community composition in bench-scale simulated water distribution systems and comparison with full-scale water mains. Environ Sci Technol 52, 13077–13088.

Anderson, M.J., Walsh, D.C.I., 2013. PERMANOVA, ANOSIM, and the mantel test in the face of heterogeneous dispersions: what null hypothesis are you testing? Ecol Monogr 83, 557–574.

Assaidi, A., Ellouali, M., Latrache, H., Mabrouki, M., Hamadi, F., Timinouni, M., Zahir, H., El Mdaghri, N., Barguigua, A., Mliji, E.M., 2018. Effect of temperature and plumbing materials on biofilm formation by Legionella pneumophila serogroup 1 and 2–15. J Adhes Sci Technol 32, 1471–1484.

Bai, X., Wu, F., Zhou, B., Zhi, X., 2010. Biofilm bacterial communities and abundance in a full-scale drinking water distribution system in Shanghai. J Water Health 8, 593–600.

Barberán, A., Bates, S.T., Casamayor, E.O., Fierer, N., 2012. Using network analysis to explore co-occurrence patterns in soil microbial communities. ISME J. 6, 343–351.

Belardinelli, J.M., Li, W., Martin, K.H., Zeiler, M.J., Lian, E., Avanzi, C., Wiersma, C.J., Nguyen, T.V., Angala, B., de Moura, V.C.N., Jones, V., Borlee, B.R., Melander, C., Jackson, M., 2022. 2-aminoimidazoles inhibit mycobacterium abscessus biofilms in a zinc-dependent manner. Int J Mol Sci 23.

Boe-Hansen, R., Albrechtsen, H.J., Arvin, E., Jorgensen, C., 2002. Bulk water phase and biofilm growth in drinking water at low nutrient conditions. Water Res 36, 4477–4486.

Bolyen, E., Rideout, J.R., Dillon, M.R., Bokulich, N., Abnet, C.C., Al-Ghalith, G.A., Alexander, H., Alm, E.J., Arumugam, M., Asnicar, F., Bai, Y., Bisanz, J.E., Bittinger, K., Brejnrod, A., Brislawn, C.J., Brown, C.T., Callahan, B.J., Caraballo-Rodriguez, A.M., Chase, J., Cope, E.K., Da Silva, R., Diener, C., Dorrestein, P.C., Douglas, G.M., Durall, D.M., Duvallet, C., Edwardson, C.F., Ernst, M., Estaki, M., Fouquier, J., Gauglitz, J.M., Gibbons, S.M., Gibson, D.L., Gonzalez, A., Gorlick, K., Guo, J., Hillmann, B., Holmes, S., Holste, H., Huttenhower, C., Huttley, G.A., Janssen, S., Jarmusch, A.K., Jiang, L., Kaehler, B.D., Bin Kang, K., Keefe, C.R., Keim, P., Kelley, S.T., Knights, D., Koester, I., Kosciolek, T., Kreps, J., Langille, M.G. I., Lee, J., Ley, R., Liu, Y.-X., Loftfield, E., Lozupone, C., Maher, M., Marotz, C., Martin, B.D., McDonald, D., McIver, L.J., Melnik, A.V., Metcalf, J.L., Morgan, S.C., Morton, J.T., Naimey, A.T., Navas-Molina, J.A., Nothias, L.F., Orchanian, S.B., Pearson, T., Peoples, S.L., Petras, D., Preuss, M.L., Pruesse, E., Rasmussen, L.B., Rivers, A., Robeson, M.S., II, Rosenthal, P., Segata, N., Shaffer, M., Shiffer, A., Sinha, R., Song, S.J., Spear, J.R., Swafford, A.D., Thompson, L.R., Torres, P.J., Trinh, P., Tripathi, A., Turnbaugh, P.J., Ul-Hasan, S., vander Hooft, J.J.J., Vargas, F., Vazquez-Baeza, Y., Vogtmann, E., von Hippel, M., Walters, W., Wan, Y., Wang, M., Warren, J., Weber, K.C., Williamson, C.H.D., Willis, A.D., Xu, Z.Z., Zaneveld, J.R., Zhang, Y., Zhu, Q., Knight, R., Caporaso, J.G., 2019. Reproducible, interactive, scalable and extensible microbiome data science using QIIME 2. Nat Biotechnol 37, 852–857.

Callahan, B.J., McMurdie, P.J., Rosen, M.J., Han, A.W., Johnson, A.J.A., Holmes, S.P., 2016. DADA2: High-resolution sample inference from Illumina amplicon data. Nat Methods 13, 581-+.

Costerton, J.W., Lewandowski, Z., Caldwell, D.E., Korber, D.R., Lappin-Scott, H.M., 1995. Microbial Biofilms. Annual Reviews in Microbiology 49, 711–745.

Cruz, M.C., Woo, Y., Flemming, H.-C., Wuertz, S., 2020. Nitrifying niche differentiation in biofilms from full-scale chloraminated drinking water distribution system. Water Res 176.

Dai, Z., Sevillano-Rivera, M.C., Calus, S.T., Bautista-de los Santos, Q.M., Eren, A.M., van der Wielen, P.W.J.J., Ijaz, U.Z., Pinto, A.J., 2020. Disinfection exhibits systematic impacts on the drinking water microbiome. MICROBIOME 8.

De Sotto, R., Tang, R., Bae, S., 2020. Biofilms in premise plumbing systems as a double-edged sword: microbial community composition and functional profiling of biofilms in a tropical region. J. Water Health 18, 172–185.

Deng, Y., Jiang, Y.H., Yang, Y.F., He, Z.L., Luo, F., Zhou, J.Z., 2012. Molecular ecological network analyses. BMC Bioinf 13.

Dixon, P., 2003. VEGAN, a package of R functions for community ecology. J Veg Sci 14, 927–930.

Douterelo, I., Sharpe, R.L., Boxall, J.B., 2013. Influence of hydraulic regimes on bacterial community structure and composition in an experimental drinking water distribution system. Water Res 47, 503–516.

Douterelo, I., Jackson, M., Solomon, C., Boxall, J., 2016. Microbial analysis of in situ biofilm formation in drinking water distribution systems: implications for monitoring and control of drinking water quality. Appl Microbiol Biotechnol 100, 3301–3311.

Douterelo, I., Jackson, M., Solomon, C., Boxall, J., 2017. Spatial and temporal analogies in microbial communities in natural drinking water biofilms. Sci Total Environ 581, 277–288.

Douterelo, I., Fish, K.E., Boxall, J.B., 2018. Succession of bacterial and fungal communities within biofilms of a chlorinated drinking water distribution system. Water Res 141, 74–85.

Dowdell, K., Haig, S.-J., Caverly, L.J., Shen, Y., LiPuma, J.J., Raskin, L., 2019. Nontuberculous mycobacteria in drinking water systems – the challenges of characterization and risk mitigation. Curr. Opin. Biotechnol. 57, 127–136.

Falkinham III, J.O., Hilborn, E.D., Arduino, M.J., Pruden, A., Edwards, M.A., 2015. Epidemiology and ecology of opportunistic premise plumbing pathogens: legionella pneumophila, Mycobacterium avium, and Pseudomonas aeruginosa. Environ Health Perspect 123, 749–758.

Fang, J., Dai, Z., Li, X., van der Hoek, J.P., Savic, D., Medema, G., van der Meer, W., Liu, G., 2023. Service-lines as major contributor to water quality deterioration at customer ends. Water Res 241.

Fayle, T.M., Turner, E.C., Foster, W.A., 2013. Ant mosaics occur in SE asian oil palm plantation but not rain forest and are influenced by the presence of nest-sites and non-native species. Ecography 36, 1051–1057.

Feng, K., Zhang, Z., Cai, W., Liu, W., Xu, M., Yin, H., Wang, A., He, Z., Deng, Y., 2017. Biodiversity and species competition regulate the resilience of microbial biofilm community. Mol. Ecol. 26, 6170–6182.

Fierer, N., Jackson, J.A., Vilgalys, R., Jackson, R.B., 2005. Assessment of soil microbial community structure by use of taxon-specific quantitative PCR assays. Appl Environ Microbiol 71, 4117–4120.

Gomez-Smith, C.K., LaPara, T.M., Hozalski, R.M., 2015. Sulfate reducing bacteria and mycobacteria dominate the biofilm communities in a chloraminated drinking water distribution system. Environ Sci Technol 49, 8432–8440.

Guimerà, R., Nunes Amaral, L.A., 2005. Functional cartography of complex metabolic networks. Nature 433, 895–900.

Guo, B.; Zhang, L.; Sun, H.; Gao, M.; Yu, N.; Zhang, Q.; Mou, A.; Liu, Y. Microbial co-occurrence network topological properties link with reactor parameters and reveal importance of low-abundance genera. npj Biofilms Microbiomes 2022;8:3.

Henne, K., Kahlisch, L., Brettar, I., Hoefle, M.G., 2012. Analysis of structure and composition of bacterial Core communities in mature drinking water biofilms and bulk water of a citywide network in Germany. Appl Environ Microbiol 78, 3530–3538.

Hu, D., Hong, H., Rong, B., Wei, Y., Zeng, J., Zhu, J., Bai, L., Guo, F., Yu, X., 2021. A comprehensive investigation of the microbial risk of secondary water supply systems in residential neighborhoods in a large city. Water Res 205.

Hu, B.-L., Shen, L.-D., Zheng, P., Hu, A.-H., Chen, T.-T., Cai, C., Liu, S., Lou, L.-P., 2012. Distribution and diversity of anaerobic ammonium-oxidizing bacteria in the sediments of the Qiantang River. Environ Microbiol Rep 4, 540–547.

Huang, C.K., Weerasekara, A., Bond, P.L., Weynberg, K.D., Guo, J., 2021. Characterizing the premise plumbing microbiome in both water and biofilms of a 50-year-old building. Sci Total Environ 798.

Jackson, C.R., Churchill, P.F., Roden, E.E., 2001. Successional changes in bacterial assemblage structure during epilithic biofilm development. Ecology 82, 555–566.

Jing, Z., Lu, Z., Mao, T., Cao, W., Wang, W., Ke, Y., Zhao, Z., Wang, X., Sun, W., 2021. Microbial composition and diversity of drinking water: a full scale spatial-temporal investigation of a city in northern China. Sci. Total Environ. 776, 145986.

Jousset, A., Bienhold, C., Chatzinotas, A., Gallien, L., Gobet, A., Kurm, V., Kuesel, K., Rillig, M.C., Rivett, D.W., Salles, J.F., van der Heijden, M.G.A., Youssef, N.H., Zhang, X., Wei, Z., Hol, W.H.G., 2017. Where less may be more: how the rare biosphere pulls ecosystems strings. ISME J 11, 853–862.
Ju, F., Xia, Y., Guo, F., Wang, Z., Zhang, T., 2014. Taxonomic relatedness shapes bacterial assembly in activated sludge of globally distributed wastewater treatment plants. Environ. Microbiol. 16, 2421–2432.
Kechin, A., Boyarskikh, U., Kel, A., Filipenko, M., 2017. cutPrimers: a new tool for accurate cutting of primers from reads of targeted next generation sequencing. J Comput Biol 24, 1138–1143.
Kitajima, M., Cruz, M.C., Williams, R.B.H., Wuertz, S., Whittle, A.J., 2021. Microbial abundance and community composition in biofilms on in-pipe sensors in a drinking water distribution system. Sci Total Environ 766.
Lautenschlager, K., Boon, N., Wang, Y., Egli, T., Hammes, F., 2010. Overnight stagnation of drinking water in household taps induces microbial growth and changes in community composition. Water Res 44, 4868–4877.
Learbuch, K.L.G., Smidt, H., van der Wielen, P.W.J.J., 2021. Influence of pipe materials on the microbial community in unchlorinated drinking water and biofilm. Water Res 194.
Lehtola, M.J., Miettinen, K.T., Keinanen, M.M., Kekki, T.K., Laine, O., Hirvonen, A., Vartiainen, T., Martikainen, P.J., 2004. Microbiology, chemistry and biofilm development in a pilot drinking water distribution system with copper and plastic pipes. Water Res 38, 3769–3779.
Li, J., Ren, A., van der Mark, E., Liu, G., 2022. Direct evidence of microbiological water quality changes on bacterial quantity and community caused by plumbing system. J Environ Sci 116, 175–183.
Li, W., Wang, F., Zhang, J., Qiao, Y., Xu, C., Liu, Y., Qian, L., Li, W., Dong, B., 2016. Community shift of biofilms developed in a full-scale drinking water distribution system switching from different water sources. Sci Total Environ 544, 499–506.
Li, W., Tan, Q., Zhou, W., Chen, J., Li, Y., Wang, F., Zhang, J., 2020. Impact of substrate material and chlorine/chloramine on the composition and function of a young biofilm microbial community as revealed by high-throughput 16S rRNA sequencing. Chemosphere 242.
Ling, F., Whitaker, R., LeChevallier, M.W., Liu, W.-T., 2018. Drinking water microbiome assembly induced by water stagnation. ISME J 12, 1520–1531.
Liu, G., Bakker, G., Li, S., Vreeburg, J., Verberk, J., Medema, G., Liu, W., Van Dijk, J., 2014. Pyrosequencing reveals bacterial communities in unchlorinated drinking water distribution system: an integral study of bulk water, suspended solids, loose deposits, and pipe wall biofilm. Environ. Sci. Technol. 48, 5467–5476.
Liu, G., Tao, Y., Zhang, Y., Lut, M., Knibbe, W.-J., van der Wielen, P., Liu, W., Medema, G., van der Meer, W., 2017a. Hotspots for selected metal elements and microbes accumulation and the corresponding water quality deterioration potential in an unchlorinated drinking water distribution system. Water Res 124, 435–445.
Liu, G., Zhang, Y., Knibbe, W.-J., Feng, C., Liu, W., Medema, G., van der Meer, W., 2017b. Potential impacts of changing supply-water quality on drinking water distribution: a review. Water Res. 116, 135–148.
Liu, G., Zhang, Y., van der Mark, E., Magic-Knezev, A., Pinto, A., van den Bogert, B., Liu, W., van der Meer, W., Medema, G., 2018. Assessing the origin of bacteria in tap water and distribution system in an unchlorinated drinking water system by SourceTracker using microbial community fingerprints. Water Res 138, 86–96.
Liu, G., Zhang, Y., Liu, X., Hammes, F., Liu, W.-T., Medema, G., Wessels, P., van der Meer, W., 2020. 360-degree distribution of biofilm quantity and community in an operational unchlorinated drinking water distribution pipe. Environ. Sci. Technol. 54, 5619–5628.
Lytle, D.A., Sorg, T.J., Frietch, C., 2004. Accumulation of arsenic in drinking water distribution systems. Environ. Sci. Technol. 38, 5365–5372.
Manuel, C.M., Nunes, O.C., Melo, L.F., 2007. Dynamics of drinking water biofilm in flow/non-flow conditions. Water Res. 41, 551–562.
Martiny, A.C., Jorgensen, T.M., Albrechtsen, H.J., Arvin, E., Molin, S., 2003. Long-term succession of structure and diversity of a biofilm formed in a model drinking water distribution system. Appl Environ Microbiol 69, 6899–6907.
Martiny, A.C., Albrechtsen, H.J., Arvin, E., Molin, S., 2005. Identification of bacteria in biofilm and bulk water samples from a nonchlorinated model drinking water distribution system: detection of a large nitrite-oxidizing population associated with nitrospira spp. Appl. Environ. Microbiol. 71, 8611–8617.
Mills, K.V., Paulus, H., 2001. Reversible inhibition of protein splicing by zinc ion. J Biol Chem 276, 10832–10838.
Neu, L., Hammes, F., 2020. Feeding the building plumbing microbiome: the importance of synthetic polymeric materials for biofilm formation and management. Water 12, 1774.
Norton, C.D., LeChevallier, M.W., Falkinham Iii, J.O., 2004. Survival of Mycobacterium avium in a model distribution system. Water Res. 38, 1457–1466.
Olesen, J.M., Bascompte, J., Dupont, Y.L., Jordano, P., 2007. The modularity of pollination networks. Proc. Natl. Acad. Sci. 104, 19891–19896.
Pan, R.J., Zhang, K.J., Cen, C., Zhou, X.Y., Xu, J., Wu, J.J., Wu, X.G., 2021. Characteristics of biostability of drinking water in aged pipes after water source switching: ATP evaluation, biofilms niches and microbial community transition. Environ Pollut 271.
Papciak, D., Tchorzewska-Cieslak, B., Domon, A., Wojtus, A., Zywiec, J., Konkol, J., 2019. The impact of the quality of tap water and the properties of installation materials on the formation of biofilms. WATER 11.
Peng, C.Y., Korshin, G.V., Valentine, R.L., Hill, A.S., Friedman, M.J., Reiber, S.H., 2010. Characterization of elemental and structural composition of corrosion scales and deposits formed in drinking water distribution systems. Water Res. 44, 4570–4580.
Perrin, Y., Bouchon, D., Delafont, V., Moulin, L., Hechard, Y., 2019. Microbiome of drinking water: a full-scale spatio-temporal study to monitor water quality in the Paris distribution system. Water Res 149, 375–385.
Potgieter, S., Pinto, A., Sigudu, M., Du Preez, H., Ncube, E., Venter, S., 2018. Long-term spatial and temporal microbial community dynamics in a large-scale drinking water distribution system with multiple disinfectant regimes. Water Res 139, 406.
Prest, E.I., Hammes, F., van Loosdrecht, M.C., Vrouwenvelder, J.S., 2016. Biological stability of drinking water: controlling factors, methods, and challenges. Front. Microbiol. 7.
Proctor, C.R.; Dai, D.; Edwards, M.A.; Pruden, A. Interactive effects of temperature, organic carbon, and pipe material on microbiota composition and Legionella pneumophila in hot water plumbing systems. MICROBIOME 2017;5.
Proctor, C.R., Hammes, F., 2015. Drinking water microbiology—from measurement to management. Curr. Opin. Biotechnol. 33, 87–94.
Proctor, C.R., Reimann, M., Vriens, B., Hammes, F., 2018. Biofilms in shower hoses. Water Res 131, 274–286.
Punjabi, K., Mehta, S., Chavan, R., Chitalia, V., Deogharkar, D., Deshpande, S., 2018. Efficiency of biosynthesized silver and zinc nanoparticles against multi-drug resistant pathogens. Front Microbiol 9.
Quast, C., Pruesse, E., Yilmaz, P., Gerken, J., Schweer, T., Yarza, P., Peplies, J., Gloeckner, F.O., 2013. The SILVA ribosomal RNA gene database project: improved data processing and web-based tools. Nucleic Acids Res 41, D590–D596.
Ren, H., Wang, W., Liu, Y., Liu, S., Lou, L., Cheng, D., He, X., Zhou, X., Qiu, S., Fu, L., Liu, J., Hu, B., 2015. Pyrosequencing analysis of bacterial communities in biofilms from different pipe materials in a city drinking water distribution system of East China. Appl Microbiol Biotechnol 99, 10713–10724.
Rhoads, W.J., Pruden, A., Edwards, M.K., 2017. Interactive effects of corrosion, copper, and chloramines on legionella and mycobacteria in hot water plumbing. Environ Sci Technol 51, 7065–7075.
Sasada, R., Weinstein, M., Prem, A., Jin, M., Bhasin, J., 2020. FIGARO: an efficient and objective tool for optimizing microbiome rRNA gene trimming parameters. Journal of Biomolecular Techniques: JBT 31, S2.
Simunic, U., Pipp, P., Dular, M., Stopar, D., 2020. The limitations of hydrodynamic removal of biofilms from the dead-ends in a model drinking water distribution system. Water Res 178.
Stone, L., Roberts, A., 1990. The checkerboard score and species distributions. Oecologia 85, 74–79.
Tang, W., Li, Q., Chen, L., Zhang, W.X., Wang, H., 2021. Biofilm community structures and opportunistic pathogen gene markers in drinking water mains and the role of pipe materials. ACS ES&T Water 1 (3), 630–640.
Telesford, Q.K., Joyce, K.E., Hayasaka, S., Burdette, J.H., Laurienti, P.J., 2011. The ubiquity of small-world networks. Brain Connect. 1, 367–375.
Vaerewijck, M.J.M., Huys, G., Palomino, J.C., Swings, J., Portaels, F., 2005. Mycobacteria in drinking water distribution systems: ecology and significance for human health. FEMS Microbiol. Rev. 29, 911–934.
van der Kooij, D., Bakker, G.L., Italiaander, R., Veenendaal, H.R., Wullings, B.A., 2017. Biofilm composition and threshold concentration for growth of legionella pneumophila on surfaces exposed to flowing warm tap water without disinfectant. Appl Environ Microbiol 83, e02737–e12716.
Waak, M.B., LaPara, T.M., Halle, C., Hozalski, R.M., 2018. Occurrence of legionella spp. in water-Main biofilms from two drinking water distribution systems. Environ Sci Technol 52, 7630–7639.
Waak, M.B., LaPara, T.M., Halle, C., Hozalski, R.M., 2019. Nontuberculous mycobacteria in two drinking water distribution systems and the role of residual disinfection. Environ Sci Technol 53, 8563–8573.
Wang, H., Edwards, M., Falkinham III, J.O., Pruden, A., 2012. Molecular survey of the occurrence of legionella spp., mycobacterium spp., Pseudomonas aeruginosa, and amoeba hosts in two chloraminated drinking water distribution systems. Appl Environ Microbiol 78, 6285–6294.
Wang, H., Masters, S., Edwards, M.A., Falkinham III, J.O., Pruden, A., 2014. Effect of disinfectant, water age, and pipe materials on bacterial and eukaryotic community structure in drinking water biofilm. Environ Sci Technol 48, 1426–1435.
Wang, H., Bedard, E., Prevost, M., Camper, A.K., Hill, V.R., Pruden, A., 2017. Methodological approaches for monitoring opportunistic pathogens in premise plumbing: a review. Water Res 117, 68–86.
Wu, H.T., Zhang, J.X., Mi, Z.L., Xie, S.G., Chen, C., Zhang, X.J., 2015. Biofilm bacterial communities in urban drinking water distribution systems transporting waters with different purification strategies. Appl Microbiol Biotechnol 99, 1947–1955.
Xu, R., Yu, Z., Zhang, S., Meng, F., 2019. Bacterial assembly in the bio-cake of membrane bioreactors: stochastic vs. deterministic processes. Water Res 157, 535–545.
Yang, X., Beyenal, H., Harkin, G., Lewandowski, Z., 2000. Quantifying biofilm structure using image analysis. J Microbiol Methods 39, 109–119.
Yao, M., Zhang, Y., Dai, Z., Ren, A., Fang, J., Li, X., van der Meer, W., Medema, G., Rose, J.B., 2023. Liu, G. Influences of premise plumbing configuration. Water Res, Building water quality deterioration during water supply restoration after interruption, p. 241.
Yu, J., Kim, D., Lee, T., 2010. Microbial diversity in biofilms on water distribution pipes of different materials. Water Sci Technol 61, 163–171.
Zhang, G., Li, B., Guo, F., Liu, J., Luan, M., Liu, Y., Guan, Y., 2019. Taxonomic relatedness and environmental pressure synergistically drive the primary succession of biofilm microbial communities in reclaimed wastewater distribution systems. Environ. Int. 124, 25–37.
Zhang, X., Lin, T., Jiang, F., Zhang, X., Wang, S., Zhang, S., 2022. Impact of pipe material and chlorination on the biofilm structure and microbial communities. Chemosphere 289, 133218.